P1.5

ESTIMATING THE FLUCTUATIONS IN DROPLET FALL VELOCITY VIA IN SITU MEASUREMENTS IN STRATOCUMULUS: AN ESSENTIAL STEP IN AIRBORNE DOPPLER RADAR TURBULENCE MEASUREMENTS

Marie Lothon* (1), Donald H. Lenschow(1), Dave Leon(2) and Gabor Vali(2)

(1) National Center for Atmospheric Research, Boulder, CO
(2) Department of Atmospheric Science, University of Wyoming, Laramie, WY

1. INTRODUCTION

During DYCOMS-II (the second DYnamics and Chemistry Of Marine Stratocumulus field experiment), the stratocumulus-topped boundary layer (STBL) was probed off the coast of southern California, in order to better understand the physics and dynamics of the persistent stratocumulus found there during summer (see the overview of the resources and objectives of this experiment presented by Stevens et al (2002)). While the NCAR C-130 aircraft was flying 60 km diameter quasi-Lagrangian circles at different levels in the STBL and in the overlying free troposphere, the 95 GHz (3 mm wavelength) WCR observed the cloudy atmosphere below with two downward-looking beams. The high rate sampling of the Doppler velocity measurements allowed us to attempt to study the turbulence characteristics (see 6.4 extended abstract).

Since the scatterers observed by the WCR are hydrometeors, the radial velocity measured by the radar is equal to the radial component of the air velocity plus the radial component of the fall velocity of these scatterers. The variance of a time series of mean Doppler velocity measured with the vertical beam can thus be written:

$$\sigma_{v_r}^2 = \sigma_w^2 + \sigma_{v_t}^2 + 2\,cov(w, v_t), \qquad (1)$$

where σ_w^2 and $\sigma_{v_t}^2$ are the contributions to the total fluctuations of the Doppler velocity due respectively to the air vertical velocity and to the terminal fallspeed of the scatterers, and *cov* indicates the covariance. By convention, w and v_t are taken negative downward. Our aim here is to estimate the fluctuations of the reflectivity-weighted fall velocity $\sigma_{v_t}^2$, a crucial step in the study of turbulence using the WCR Doppler velocity measurements.

We propose a way to directly estimate the terminal fall velocity variance from the drop counts in stratiform clouds, using the in situ microphysics probe measurements. The combination of in situ microphysics probe and airborne radar measurements during DYCOMS gave us an excellent opportunity to attempt it.

**corresponding author address:* Marie Lothon, National Center for Atmospheric Research, P. O. Box 3000, Boulder, CO 80307-3000; *email*: lothon@ucar.edu

2. METHOD

To study the spatial distribution of the drops (here we define drops to include all hydrometeors), we used the FSSP-100 (Forward Scattering Spectrometer Probe) for the small cloud droplets (2-47 μm), and the 260X 1D probe (10-640 μm). Both the FSSP-100 and the 260X probes had a sampling period of 0.1 s. The sparsity of the drizzle drops (200 μm to 500 μm), when observed with a microphysical instrument, makes it impossible to directly analyze the time series of the reflectivity-weighted fall velocity and deduce its turbulence structure. For a 1 s period and at an airspeed of 100 m s^{-1}, the sampling volume of the 260X probe is about 1 L and the concentration of the 200 μm drops is around 0.1 L^{-1} for a 10 μm bin width. These larger drops, however, play a crucial role in the reflectivity and Doppler velocity signal, because the reflectivity is proportional to the sixth moment of the drop diameter. Because of sampling volume issues, a more global statistical point of view is necessary to estimate the fluctuation in the reflectivity-weighted fall velocity.

The distribution of drops measured by the PMS probes is determined by two factors: the first is a result of the finite number of drops counted by the probe in each time interval and the second comes from real heterogeneities in the structure of the cloud. If the drop concentration was uniform with drops randomly distributed in space, a homogeneous Poisson distribution would be expected. However, the concentration varies in space and time. The counting is therefore a generalized Poisson process, *i.e.*, the counting rate varies along the flight path. Thus the observed distribution results from the combination of random counting statistics for a homogeneous distribution and real spatial variability in the drop time series, due to physical processes in clouds. The latter variability is needed in order to estimate the fluctuation in the fall velocity measured by the Doppler radar. We use the departure of the observed distribution of drops from a homogeneous random Poisson distribution to estimate the variance of drop counts due to physical processes and to deduce the corresponding variance of the reflectivity-weighted fall velocity.

Assuming that the two processes described above are independent, the variance in counts measured by a PMS probe in a particular bin i should be equal to the variance due to the statistical Poisson process plus the variance due to the physical cloud processes:

$$\left(\sigma^2_{n_i}\right)_{PMS-obs} = \left(\sigma^2_{n_i}\right)_{Pois} + \left(\sigma^2_{n_i}\right)_{phys}. \qquad (2)$$

Determining the set of $\left(\sigma^2_{n_i}\right)_{phys}$ for all the bins will enable us to estimate the contribution σ_{v_t} of the drop fallspeed to the Doppler velocity fluctuation. The Poisson sampling variations are taken as zero for the much larger radar volumes; furthermore, variations in the in situ-derived reflectivity and fall velocity are assumed to be representative of what the radar measures over the same averaging length.

In the next section, we present the in situ measurements and discuss the observed departure from Poisson statistics. We show that the observed count distribution can be modeled by a generalized Poisson distribution, that would have a lognormally distributed counting rate. Then we give estimates of the variance of the reflectivity-weighted fall velocity deduced from the non-Poisson variance of the counts.

3. MODELING THE COUNT DISTRIBUTION OBSERVED BY A PMS PROBE

3.1 Observed count distributions

The data presented in this paper were collected during flight RF07, which had the most uniform distribution of drizzle among the nine DYCOMS flights (Van Zanten et al., 2004). Eight legs probed the STBL, two at each of the four levels flown: near cloud top (CT1 and CT2), just above cloud base (CB1 and CB2), between cloud base and the surface (SC1 and SC2) and 95 m above the surface (SF1 and SF2). The height of the legs, cloud base and cloud-top heights are listed in Table 1. Each leg consisted of a 60 km diameter circle flown within about 30 minutes. At each level, circles were flown both clockwise and anti-clockwise. The drop size distributions observed were bimodal (Van Zanten et al., 2004). One mode was composed of the small cloud droplets with a median diameter of about 20 μm and the other of larger drops, including drizzle, with a median diameter of about 100 μm. The small cloud droplet concentration was as much as 10^5 times larger than the drizzle concentration at cloud top but more like 10^2 times larger in the sub-cloud region. We mainly used the 260X measurements because the contribution of the small cloud droplets (measured with the FSSP-100) to the reflectivity turned out to be negligible. Drizzle was prevalent during this flight and made the largest contribution to the observed reflectivity and the reflectivity-weighted fall velocity. The counts were accumulated over a sampling interval of 2 s (about 200 m) as a compromise between obtaining a sufficient count rate and resolving turbulence structure. Both legs at each level were used together, so that the number of sampling intervals (N_{dp}) was 1800.

	GPS altitude (m.s.l)
Cloud base	275
Cloud top	825
CT1	712
CT2	677
CB1 and CB2	448
SC1 and SC2	230
SF1 and SF2	95

Table 1: *Height of cloud top, cloud base and of the legs flown during flight RF07 of DYCOMS-II*

Figure 1 displays the frequency of counts per 2 s period observed for the 115 μm channel of the 260X probe on the CB leg, along with the frequency of counts expected for a Poisson distribution of the same rate (the rate $\bar{n}$ is the ratio of the total number of events to the number of sampling intervals). The measured distributions depart from a Poisson distribution. A standard test based on the chi-square distribution (Hogg and Tanis, 1993) allowed us to quantify the significance of this departure and reject the null hypothesis that the counts are Poisson-randomly distributed at the 1% significance level.

The departure from Poisson randomness can also be quantified using the clustering index (*i.e* Barker,1992):

$$CI = \frac{\overline{(\delta n)^2}}{\bar{n}} - 1, \qquad (3)$$

where $\overline{(\delta n)^2}$ is the variance of the counts. Since the variance and the mean are equal for a Poisson distribution, CI$= 0$ for Poisson statistics. Positive CI implies a more clustered distribution while negative CI implies a more uniform distribution than Poisson. Table 2 displays the characteristics of the count distribution for the 195 μm channel with a 2 s sampling interval. The clustering index we observe is positive, consistent with the excess of 'zero count' events relative to the Poisson distribution, along with a depletion of one and two count events, displayed in Fig. 1.

3.2 Modeling the observed distribution

Here we show that the departure from Poisson statistics discussed above can be explained by a lognormal spatial distribution due to physical processes. Therefore,

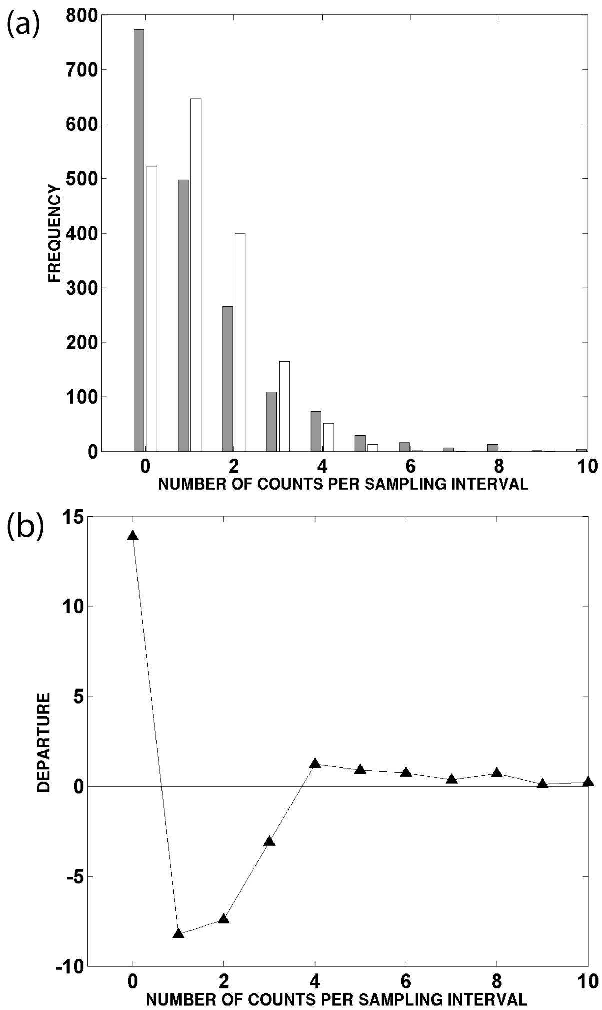

Figure 1: *(a) frequency of counts observed (shaded) at 2 s sampling time interval in the 115 µm channel of the 260X probe for CB, along with the frequency of counts expected for a Poisson distribution with the same mean number of counts per sampling time interval (unshaded). (b) observed minus expected Poisson probability density function (times 100).*

LEG	λ	N_{tot}	$\overline{n}$	$\overline{(\delta n)^2}$	CI
CT	0.116	209	0.247	0.423	0.71
CB	0.131	236	0.660	1.393	1.11
SC	0.144	260	0.305	0.405	0.33
SF	0.065	111	0.137	0.219	0.60

Table 2: *Characteristics of the count distribution for the 195 µm channel, at the 4 levels probed during flight RF07 and for a 2 s sampling period. λ is the mean count rate (s^{-1}), N_{tot} is the total number of counts, $\overline{n}$ is the mean number of counts per sampling period, $\overline{(\delta n)^2}$ the variance of the counts and CI is the clustering index (equation (3)).*

we make use of the concept of a doubly stochastic process to describe the Poisson random sampling of counts which, in addition, have a spatial distribution due to cloud heterogenities, in order to model the distribution observed by the microphysics probes. This concept is similar to the 'Poisson mixture' approach used by Kostinski and Jameson (1997), but we assume a lognormally varying Poisson distribution (LVPD). The model we propose to explain and quantify the departure from a Poisson distribution is based on the assumption that, instead of a constant rate $\overline{n}_i$, the expected count distribution in each size bin i has a variable rate with a lognormal distribution. The variance $\sigma^2_{n_i}$ of this lognormal distribution characterizes the variance of the actual heterogeneities of a particular bin. We can then quantify the variance of the overall fall velocity obtained from all the bins as described in the next section.

At low sampling rates (i.e. large drops), the mean number of counts per time interval may be very small (see Table 2), so a Gaussian distribution is not appropriate because of negative values. Our choice of a lognormal distribution differs from the exponential distribution chosen by Kostinski and Jameson (1997) for raindrops. However, the lognormal distribution has previously been used to describe scalars in the atmosphere (*e.g.*, Hogan and Illingworth (2003) or Titov and Kas'yanov (1995)) and in their study of coastal stratus clouds, Vali et al. (1998) found that the distribution of reflectivity measured by the WCR was well approximated by a lognormal distribution (normal distribution in dBZ). We generally obtained the same result in DYCOMS-II.

The lognormal distribution is estimated as follows: For each bin i, a random series is generated based on a Poisson process, but using a lognormally-distributed rate, with a mean $\overline{n}_i$ and a standard deviation σ_{n_i} (see Appendix for the probability density function (PDF) of the Poisson and lognormal distributions). $\overline{n}_i$ is taken equal to the observed mean number of counts per time interval and σ_{n_i} is chosen to best fit the observed distribution.

To determine the value of σ_{n_i} which best fits the observations for each leg using a sampling interval of 2 s, the squared differences between the observed and modeled departure were plotted as a function of σ_{n_i}. For each leg, the LVPDs were generated with $\overline{n}_i$ equal to the mean number of counts observed. Figure 2 displays the results for the 115 μm binsize at CB and shows that there is an objective way to optimize the estimate of σ_{n_i}; i.e. the value of σ_{n_i} which minimizes the squared difference. Figures 3 displays, for the same leg and binsize, the observed and modeled departure for the optimal σ_{n_i}. The agreement is very convincing, and it was generally the case for all bins of the 260-X probe and for all legs.

The variance of the counts that we obtain from the LVPD approach is an estimate of the variance due to hor-

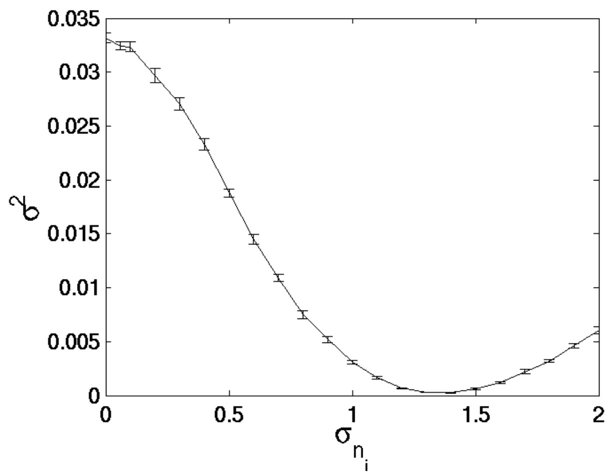

Figure 2: *Squared difference between the observed departure from random Poisson statistics σ^2 and the modeled departure as a function of the standard deviation of counts σ_{n_i}, for the case of 115 μm bin size at CB. Note that σ^2 was usually one or two orders of magnitude larger than that found for two random Poisson series of same rate. The vertical barred line represent the variation over 100 cases.*

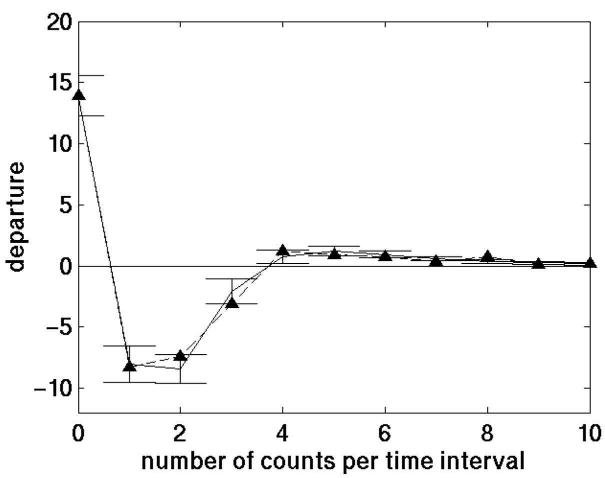

Figure 3: *Observed (triangles and dashed line) and modeled (solid line) departure from random Poisson statistics (times 100) in the 115 μm channel at CB, for the σ_{n_i} value which minimizes the error shown in Fig. 2. The vertical barred lines represent the standard deviation of 100 cases.*

izontal heterogeneities in the drop distribution. The variance calculated directly from a series of counts is the variance due to Poisson counting process (equal to the mean number of counts) plus the non-Poisson variance contributed by the heterogeneities, since the two processes should be independent (see eq. 2). Figure 4 shows the sum of the Poisson variance ($\overline{n}_i$) plus the variance due to the lognormal distribution ($\sigma^2_{n_i}$), versus the total variance calculated directly ($\overline{\delta n^2}_i$). The one-to-one slope suggests good agreement between the two estimates of the total variance. This confirms our assumption that the two processes are independent and lends further support to our selection of a lognormally varying Poisson process.

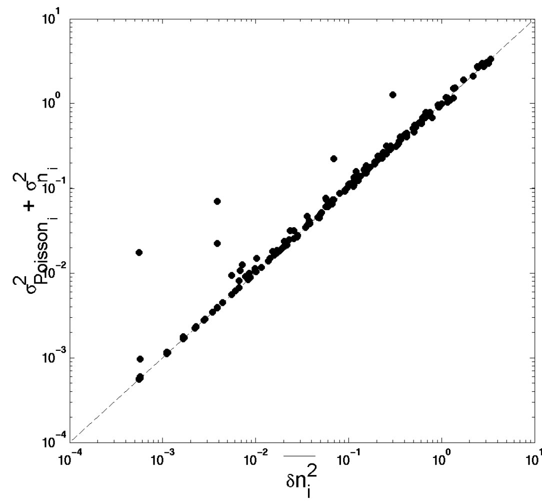

Figure 4: *Sum of the variance in counts calculated from a Poisson random process plus lognormally-distributed cloud heterogeneities versus the total variance obtained directly from the counts. All the legs and bins are considered here, one point representing one bin in a given leg. The probe used is the 260X. Note the logarithmic scale.*

4. ESTIMATING DOPPLER VELOCITY FLUCTUATIONS

In order to evaluate the effect of the fall velocity fluctuations on the variance of the Doppler velocity, we need to estimate the standard deviation of the reflectivity-weighted fall velocity from the standard deviation of the counts in each bin due to physical processes, that was evaluated using the method shown in the previous section.

The reflectivity and the reflectivity-weighted fall velocity resulting from the drops measured by the PMS probe are:

$$Z(j) = \sum_i c_i(j) D_i^6, \tag{4}$$

$$v_{t_z}(j) = \frac{\sum_i c_i(j) v_{t_i} D_i^6}{\sum_i c_i(j) D_i^6}. \quad (5)$$

The summation is over all the bins, D_i is the diameter of drops in bin i, v_{t_i} is the terminal fall velocity of the drops of size D_i, c_i is the concentration of drops in the same bin, and j is the time or space counter. The 260X bin drop sizes ranged from 15 to 645 μm with a width of 10 μm. c_i is deduced from the number of counts n_i by

$$c_i(j) = \frac{n_i(j)}{V_a(j)\Delta t\, S_i}, \quad (6)$$

where V_a is the aircraft true airspeed, Δt is the sampling period and S_i is the PMS sampling area. The terminal fall velocity of the particle as a function of diameter is given by (Rogers and Yau, 1989):

$$v_{t_i}(D_i) = -0.3\ 10^8\, Di^2 \quad \text{for } D_i \leq 133\,\mu\text{m},$$
$$v_{t_i}(D_i) = -4.0\ 10^3\, Di \quad \text{for } 133\,\mu\text{m} < D_i \leq 1250\,\mu\text{m}. \quad (7)$$

The variance of the reflectivity and of the fall velocity was computed by a simple numerical model. Random lognormal distributions of counts with 10^5 sample intervals were generated for each bin, using the mean number $\overline{n}_i$ and standard deviation of counts σ_{n_i}, and were used to calculate a random series of Z and v_{t_z} with equations (4) and (5). Because of the sumation over all the bins in equations (4) and (5), we had to make an assumtion relative to the way the bins fluctuate relatively to each other. The two following extreme opposite assumptions were tested: either the bins are totally independant or they are fully correlated. With the in-phase hypothesis, we found the best comparison between this calculated reflectivity variance and the observed one with the radar measurements made during a leg flown above the cloud to allow the observation of the whole cloud layer, during the same flight. Fig. 5 displays the profile of the radar reflectivity variance observed during this radar leg (after a 2 s average), compared with the calculated reflectivity variance.

The standard deviation of the reflectivity-weighted fall velocity was calculated using the same assumption. The order ($\sim$ 0.05 ms^{-1}) found is small relative to standard deviation of the vertical Doppler velocity observed with the radar ($\sim$ 0.4 ms^{-1}) at the same scale. Because the fall velocity variance is an order of magnitude less than the air vertical velocity variance, this variance will not have a strong impact on the study of turbulence from the Wyoming Cloud Radar Doppler velocity during this flight. Since the reflectivity-weighted fall velocity is insensitive to any fluctuation in the total number of particles, provided the size distribution function stays the same, the small order of magnitude we find for the reflectivity-weighted

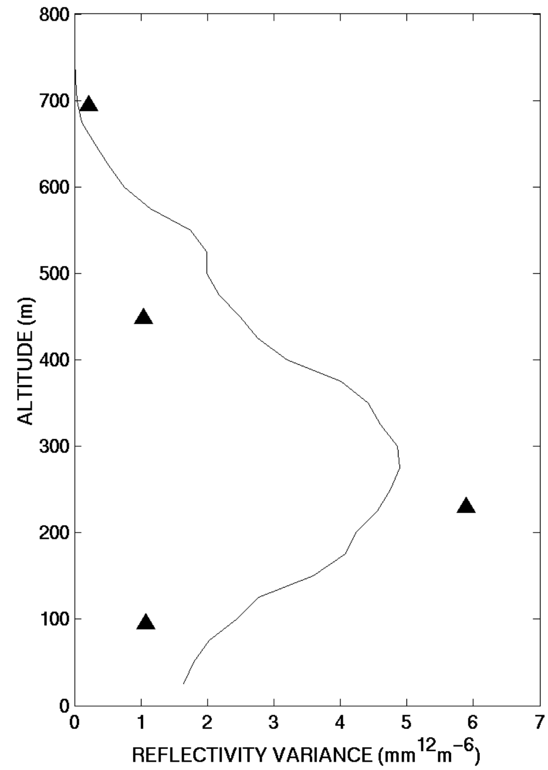

Figure 5: *Reflectivity variance profile. Solid line: profile of the radar reflectivity variance over the whole radar leg, obtained from 2 s averaged measurements. Closed triangles: reflectivity variance deduced from the 260X measurements, with the assumption that the bins are in phase.*

fall velocity is consistent with the results of Van Zanten et al. (2004) who observed that the normalized drop size distribution (median diameter and width) from 2 minute time intervals hardly changes along the leg, while the total number of particles does change. Using radar reflectivity measurements during the East Pacific Investigation of Climate (EPIC), Comstock et al. (2003) deduced the median radius $\overline{r}$ and the total number of drizzle drops N_D from Z-R relationships and made the same observation; that is the fluctuations in precipitation rate are primarily determined by the fluctuations in N_D.

5. CONCLUDING REMARKS

We find that the assumption of a lognormal horizontal distribution of hydrometeors in marine stratocumulus combined with Poisson-distributed fluctuations in the observed count rate due to the limited sampling volume gives good agreement with the observed count distributions for the 260X probe.

We were able to deduce the variance of the reflectivity-weighted fall velocity from the non-Poisson variance of the counts in each bin. This residual variance is due to physical cloud processes. For the purpose of using Doppler velocity measurements to study the characteristics of the turbulence in stratocumulus (see extended abstract 6.4) and as a first step in this study, we found a relatively small variance of the reflectivity-weighted fall velocity compared with the vertical air velocity.

Most of the limitations of this study are due to the sparsity of the drizzle drops and the difficulty in measuring them. In addition, there may be some heterogeneities of the microphysics structure at smaller scales that are likely not accurately modeled by a simple lognormal distribution. These limitations lead to larger uncertainties in our estimate of the fluctuation in reflectivity-weighted fall velocity.

APPENDIX

Poisson probability density function

Given the mean number of counts per sampling time interval $\overline{n}$, the Poisson probability density function is the probability of observing k counts during a particular time interval:

$$P(k) = \frac{\overline{n}^k}{k!} e^{-\overline{n}}. \tag{8}$$

The variance and the mean of a Poisson distribution are equal.

Lognormal distribution

A random variable n has a lognormal distribution if $\ln n$ has a normal distribution. The lognormal distribution is a two-parameter distribution with parameters μ' and $\sigma_{n'}$, where μ' is the mean of $\ln n$, and $\sigma_{n'}$ is the standard deviation of $\ln n$. The lognormal probability density function is

$$f(n) = \frac{1}{n\sigma_{n'}\sqrt{2\pi}} e^{-\frac{1}{2}\left(\frac{\ln n - \mu'}{\sigma_{n'}}\right)^2}. \tag{9}$$

Defining $\overline{n}$ and σ_n as respectively the mean and the standard deviation of n, we have:

$$\begin{aligned} \mu' &= \ln\overline{n} - \frac{1}{2}\ln\left(\frac{\sigma_n^2}{\overline{n}^2} + 1\right) \\ \sigma_{n'} &= \sqrt{\ln\left(\frac{\sigma_n^2}{\overline{n}^2} + 1\right)} \end{aligned} \tag{10}$$

Acknowledgements

Support for the DYCOMS-II project was provided by NSF Grant ATM-0097053 and ATM-0094956. NSF and ONR provided major funding for the acquisition, development and research use of the Wyoming Cloud Radar. This work was made possible thanks to ASP, MMM and ATD divisions of NCAR, the University of Wyoming and the Ministry of Foreign Affairs of France that provided a BFE Lavoisier grant to the first author during a postdoctoral fellowship.

REFERENCES

Barker, H. W., 1992: Solar radiative transfer through clouds processing isotropic variable extinction coefficient, *Q. J. R. Meteorol. Soc.*, **118**, 1145–1162.

Comstock, K. K., R. Wood, S. E. Yuter, and C. S. Bretherton, 2003: Reflectivity and rain rate in and below drizzling stratocumulus, *submitted to the Q. J. R. Meteorol. Soc.*

Hogan, R. J. and A. J. Illingworth, 2003: Parameterizing ice cloud inhomogeneity and the overlap of inhomogeneities using cloud radar data, *J. Atmos. Sci.*, **60**, 756–767.

Hogg, R. V. and E. A. Tanis, 1993: *Probability and statistical inference*, Macmillan Publishing Company, 731 pp.

Kostinski, A. B. and A. R. Jameson, 1997: Fluctuation properties of precipitation. Part I: On deviations of single-size drop counts from the Poisson distribution, *J. Atmos. Sci.*, **54**, 2174–2186.

Rogers, R. R. and M. K. Yau, 1989: *A short course in cloud physics*, Butterworth Heinemann, 290 pp.

Stevens, B. et al, 2002: Dynamics and Chemistry of Marine Stratocumulus – DYCOMS-II, *Bull. Am. Meteorol. Soc.*, **84**, 579–593.

Titov, G. A. and Y. I. Kas'yanov, 1995: Solar radiation fluxes in inhomogeneous stratus, *Optika atmosfery i okeana*, **8**, 1833–1842.

Vali, G., R. Kelly, J. French, S. Haimov, D. Leon, R. McIntosh, and A. Pazmany, 1998: Finescale structure and microphysics of coastal stratus, *J. Atmos. Sci.*, **55**, 3540–3564.

Van Zanten, M. C., B. Stevens, G. Vali, and D. H. Lenschow, 2004: On drizzle rates in nocturnal marine stratocumulus, *Accepted at J. Atmos. Sci.*